Concentration-Dependent Br···O Halogen Bonding between Carbon Tetrabromide and Oxygen-Containing Organic Solvents

Wen Sheng Zou, Juan Han, and Wei Jun Jin*

College of Chemistry, Beijing Normal University, Beijing 100875, People's Republic of China

Received: June 24, 2009; Revised Manuscript Received: August 2, 2009

High concentration-dependent halogen bonding, a specific solvent effect between carbon tetrabromide and oxygen-containing organic solvents, including methanol, ethanol, acetone, dioxane, diethyl ether, and tetrahydrofuran, was found to coexist with the general solvent effect when CBr_4 was over 7.8×10^{-3} M $\sim$ 1.6×10^{-2} M critical concentration range. In contrary, in less than this concentration range, only general solvent effect occurred. The 1:1 stoichiometry of halogen bonding complex between CBr_4 and charge donor was testified using the modified Benesi−Hildebrand method. The Mulliken correlation confirmed the charge-transfer (CT) character of the CBr_4/solvent associations. The electronic coupling elements (H_{DA}) showed that the C−Br···O complexes are most-likely localized, which is named as outer-type complex. Density functional theory (DFT) calculation was performed to predict geometry, surface electrostatic potential, interaction energy, and vibrational frequency in gas phase. The MP2 method was also employed to calculate the formation of the σ-hole (σ_h) bonding complexes between carbon tetrabromide and oxygen-containing organic solvents. The vertical excitation energies of the σ_h-bonding complexes were calculated by time-dependent density functional theory (TD-DFT). The experimental and theoretical results showed that σ_h bonding might be a more important factor for the halogen bonding complex investigated here than the CT. The results showed that Br···O halogen bonding is a blue-shift type.

1. Introduction

It has been known for a long time that the organic halogen atoms can function as Lewis acids to participate in the interaction with those atoms containing lone electron pairs such as nitrogen, oxygen, phosphorus, and sulfur, and π electron or anion in organic solvents, crystals or gas phases.[1,2] This interaction is currently named as halogen bonding (XB) as suggested by Legon to emphasize the similarity with hydrogen bonding (HB),[3,4] also named as σ-hole (σ_h) bonding based on the calculation of atomic/molecular surface electrostatic potentials.[2,5−11] In the recent decade, the research on XB has become an attractive field involving materials science, biology, drug design, and so forth. New crystal or liquid crystal materials have been prepared using the XB principle.[12−22] Much attention has been paid toward new insights of interactions of halogenated biomolecules or drugs as ligands with their protein receptors.[23−25] Theoretically, the nature of halogen bonding has been explored well and some models including electrostatic attraction plus dispersion based on anisotropy distribution of electron density,[26−30] the charger-transfer (CT) interaction,[31] and σ_h bonding[5−11] are sequentially presented. Among them, σ_h bonding should be favorable. According to Politzer's viewpoint,[7,10] when a half-filled p orbital participates in forming a covalent bond, its electron normally tends to be somewhat localized in internuclear region, thereby diminishing the electronic density in the outer (noninvolved) lobe of that orbital. This electron-deficient outer portion of a half-filled p-bonding orbital is called a "σ_h" which can accept or attract the negatively charged species. In the σ_h-bonding model, the halogen atom acts as either charge donor in the negatively charged ring region around C-halogen axial or acceptor in the positively charged region of outer center of C-halo axial direction. The σ_h, in fact, is a result from anisotropic distribution of electronic density of bound halogen atom and σ_h bonding is actually the electrostatic attraction between positive σ_h and electronegative species. The CT between donor and acceptor species or electrostatic attraction between positively and negatively charged species are well-recognized patterns. The CT model goes seemingly well in the explanation of the experimental absorption spectroscopy and determination of bonding constants of XB complex as described by Kochi.[31] Moreover, the directionality and geometry of XB, as well as special halogen−halogen interaction,[32,33] were confirmed by the single-crystals data.[31,34,35] The CT theory gives good explanation of the excited states of XB complex, while the σ_h-bonding model emphasizes the ground state nature and also can predict the high directionality of halogen bonding and explain triangle halogen−halogen interaction.[32,33] However, the calculation carried out by Hozba et al.[11] shows that in some conditions the electrostatic and dispersion attraction contribute together to halogen bonding; even the dispersion force could account for 61% of the overall attraction in Cl···O halogen bonding in chloroform formaldehyde dimer. So, any single pattern may not solely attribute the intrinsic characters of halogen bonding.

The weak noncovalent interaction in solution appears to be more important because the interaction affects the direction or rate of chemical or biological reactions.[36,37] The interaction between solutes and solvents, whatever involving in general or specific one, may largely influence the reaction direction or three-dimension structures of biological molecules. So, during recent years, the XB in solution also has been of strong focus.[38−40] Moreover, halogen bonds involving carbonyl or hydroxyl oxygen as the acceptors are particularly interesting in biochemistry because they are the most common types of halogen bonds involved in protein−ligand interactions. In

* Corresponding author. E-mail: wjjin@bnu.edu.cn. Phone/Fax: +86−10−58802146.

10.1021/jp905914q CCC: $40.75
Published on Web 08/25/2009

current study, the concentration-dependent Br···O halogen bonding is observed between carbon tetrabromide with six oxygen-containing organic solvents: methanol, ethanol, acetone, tetrahydrofuran (THF), diethyl ether, and dioxane. Our results obtained in experiments show that the general solvent effect occurred between carbon tetrabromide and oxygen-containing solvents only at low concentration of CBr_4, while the specific halogen bonding analogous to hydrogen bonding, occur at high CBr_4 concentration. The data from UV−Vis absorption spectroscopy and cyclic voltammetry (CV) indicate the Mulliken correlations of CT energy. Also, small electronic coupling elements show location distribution of electronic density of the XB complexes. The surface electrostatic potential of Br in CBr_4, halogen-bonding energy and geometry of complex are calculated to understand more deeply the nature of XB complex based on σ_h bonding and the CT characteristics. Meanwhile, the calculations indicate that blue-shifted halogen bonding occurred between CBr_4 and solvents investigated.

2. Experimental Section

2.1. Reagents. Carbon tetrabromide of 99% was purchased from Tokyo Chemical Industry Co., Ltd. Tetra-n-butylammonium hexafluorophosphate of 98% was purchased from Tianjin Alfa Aesar Reagent Company. Methanol, ethanol, acetone, dioxane, tetrahydrofuran, and diethyl ether were of absolute purity and purchased from Beijing Chemical Plant. All of the above were used as received without further purification. Other reagents were of analytical-reagent grade.

2.2. Absorption Spectra of the Carbon Tetrabromide with Solvent Complexes. All spectroscopic measurements were performed in a 2 mm quartz cuvette on a Cintra 10e UV−vis spectrometer, GBC. Freshly prepared solutions of carbon tetrabromide with a series of oxygen-containing solvents were used. Measurements were carried out under dark environment except for dioxane and tetrahydrofuran. The gradual dilution of methanol, ethanol, acetone, dioxane, tetrahydrofuran, and diethyl ether solution of carbon tetrabromide from 1.0 M to 6.0×10^{-6} M resulted in two types of spectra of XB complexes at 270−350 nm; see text. The stoichiometry of the complexes formed was determined by fitting the spot of A_{XBC} versus corresponding concentration over the range of critical concentration, and the correlation coefficients of resulting lines were greater than 0.99.

2.3. Electrochemical Measurements. Cyclic voltammetry (CV) was performed on a CHI660A Electrochemical Workstation at the same sweep rate of 100 mV s^{-1} with *iR* compensation and using a convenient three-electrode system of platinum working electrode, a platinum wire auxiliary electrode, and a Ag/AgCl (saturated KCl) reference electrode. The working solution was freshly prepared in different solvent and consisted of 0.0625 M carbon tetrabromide and saturated supporting electrolyte ($NBu_4^+PF_6^-$) for CV measurements under nitrogen atmosphere and dark environment[41] to eliminate the effect of dissociated bromine. Average anodic oxidation potentials, E^o_{pa}, obtained from the cyclic voltammograms were used to plot the Mulliken correlation figure of $h\nu_{CT}$, eV, versus E^o_{pa}, V vs SCE, according to literatures.[31,42] All experiments above were carried out at room temperature.

3. Computational Methods

DFT[43] B3PW91[44,45] method together with mixed basis set was used to perform quantum chemical computations of the reactants: methanol, ethanol, aether, tetrafuran, dioxane, acetone, carbon tetrabromide, and complexes ($CH_3OH\cdots CBr_4$, $C_2H_5OH\cdots CBr_4$, $(C_2H_5)_2O\cdots CBr_4$, $C_4H_8O\cdots CBr_4$, $C_4H_8O_2\cdots CBr_4$, and $(CH_3)_2CO\cdots CBr_4$). The stationary structures and energies (E) of the reactants and complexes were fully optimized with the LANL2DZ[46] basis set for bromine and the 6-311+G(3df,2p)[47] basis set for hydrogen, carbon, and oxygen atoms. Once convergence was reached, the vibrational frequencies (ω) were computed. Furthermore, the MP2[48] method was also used to calculate ground state energies at the B3PW91 optimized geometries. The electrostatic potential of reactants were calculated by B3PW91 with the basis set 6-31+G(d). We employed time-dependent density functional theory (TD-DFT)[49] at the B3PW91/6-31+G(d) level to predicted vertical electronic excitation energies (T_v) and oscillator strengths (f), respectively. All calculations were performed by Gaussian 03 program packages.[50]

4. Results and Discussion

4.1. UV−Vis Spectra of Intermolecular Complexes. UV−Vis absorption spectra allow us to investigate the energy and bonding characteristics of intermolecular complexes between carbon tetrabromide acceptor and six charge donor oxygen-containing solvents, methanol, ethanol, acetone, tetrahydrofuran, diethyl ether, and dioxane. The primitive spectra of the CBr_4 solutions diluted from 1.0 M to 6.0×10^{-6} M in various solvents are obtained. As shown in Figure 1, as the CBr_4 concentration increases to 1 M, new bands in the range 270 to 350 nm appear gradually, and corresponding absorption intensity increases gradually. The observed absorption peaks of CBr_4 are 225 nm in methanol, 226 nm in ethanol, 221 nm in acetone, 223 nm in tetrahydrofuran, 227 nm in diethyl ether, and 240 nm in dioxane; the absorption peak shifts in different solvents are ascribed to general solvent effect. The absorption of the specific solvent effect, halogen binding, occurred at longer wavelength domain as CBr_4 concentration reaches a critical concentration. Moreover, absorption spectra are red-shifted gradually with the increase in CBr_4 concentration. That is, the general solvent effect occurred below the critical concentration, and both general and specific solvent effects occur above the critical concentration. This might indicate that the XB specific solvent effect has a feature of high concentration-dependence.

It also can be seen from Figure 1C that in the case of acetone the two absorption bands are clearly separated and the second band at 326 nm is due to XB interaction between CBr_4 and acetone molecules. In the cases of the other five solvents, the new bands observed as a spectral tail at a region longer than 255 nm overlapped largely the absorption spectra of carbon tetrabromide itself (Figure 1A,B, typically in ethanol and THF). Because of the spectral overlapping, the exact location of new bands is very difficult to be resolved. Therefore, the spectrum of specific halogen bonding had to be obtained by subtracting the spectrum of CBr_4 solution at critical concentration from total spectrum corresponding at each higher concentration. Here, 7.8×10^{-3} M is used as the critical concentration of CBr_4. The resulting differential spectra are shown in Figure 1A-sub−C-sub. It can be seen from Figure 1 that new absorption peaks of halogen bonding complexes all red-shift with the increase in CBr_4 concentration. Specifically, the red-shift range is from 277 to 295 nm in methanol, from 279 to 298 nm in ethanol, from 296 to 305 nm in tetrahydrofuran, from 295 to 311 nm in dioxane, and from 284 to 303 nm in diethyl ether. The wavelength shift between absorption of CBr_4 itself and halogen binding complex is 52 nm in methanol, 53 nm in ethanol, 55 nm in dioxane, 57 nm in diethyl ether, 73 nm in tetrahydrofuran, and 105 nm in acetone. The largest shift of 105 nm observed

in acetone may imply the specialty of carbonyl in the formation of halogen binding relative to the sp^3 hybridization oxygen atom.[23,58]

4.2. Stoichiometry of the Complexes of Carbon Tetrabromide with Six Organic Solvents. Generally speaking, the stoichiometry of the complexes of two or a multicomponent system can be determined by the Benesi−Hildebrand method if the assumption is met.[51] Herein, the Benesi−Hildebrand formulation should be modified appropriately in order to better describe the specific halogen bonding complex system. D is taken to represent the electron donor, and A is the electron acceptor; then, the equilibrium can be written as

$$D + A \rightleftharpoons D\cdot A \quad (1)$$

The equilibrium constant is then expressed as

$$K = \frac{[D\cdot A]}{[D][A]} \quad (2)$$

$$A_{XBC}(t) = \varepsilon b[D\cdot A] \quad (3)$$

If the absorption is not affected reciprocally among D, A, and D·A, then

$$A_{XBC}(0) = 0$$

For the solvent effect system investigated here,

$$[D] > > [A]$$

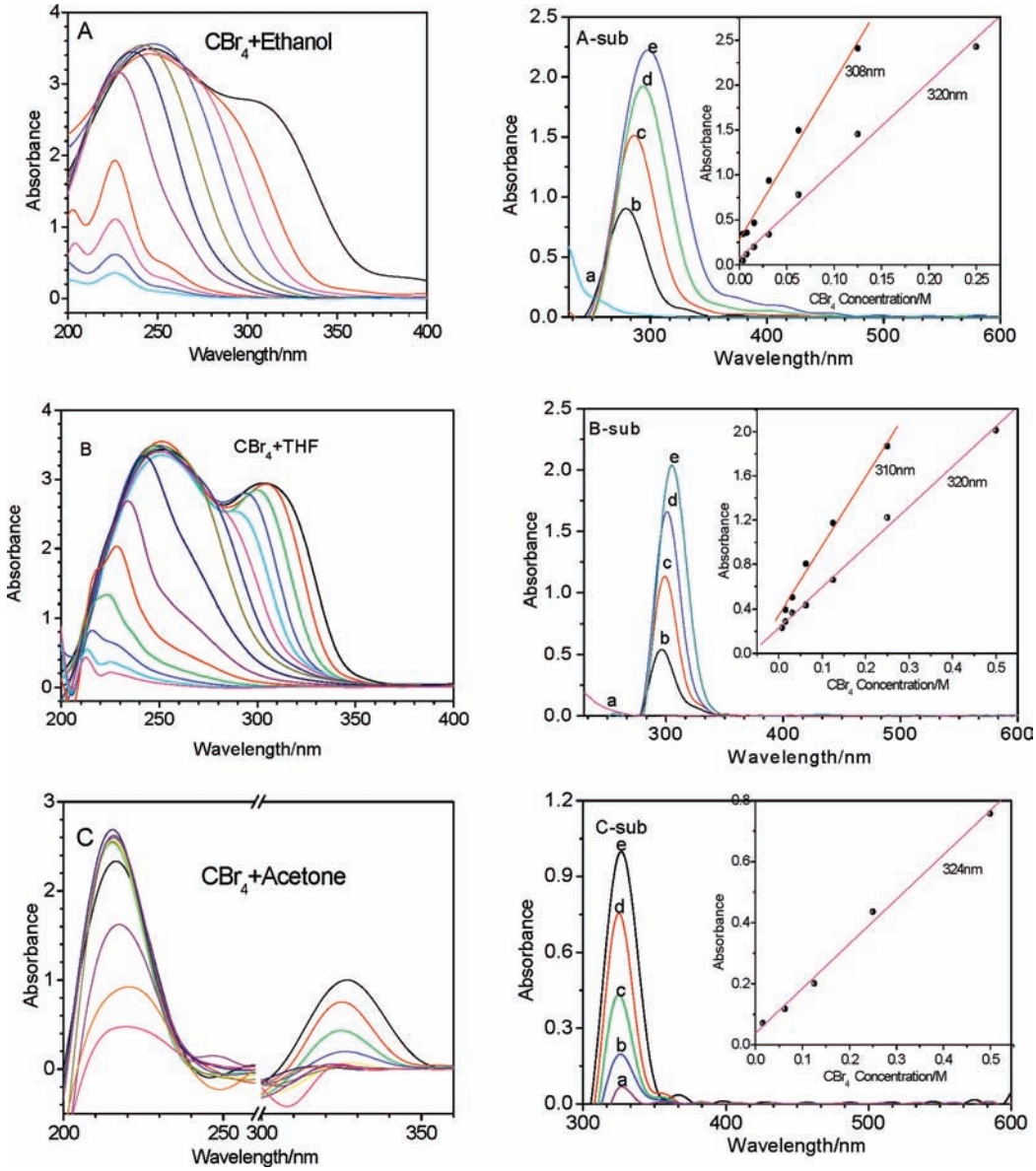

Figure 1. Typical absorption spectra (A to C) and subtracted absorption spectra (A-sub to C-sub) of halogen binding complexes between carbon tetrabromide and oxygen-containing solvents. The general and specific solvent effect, halogen bonding, are overlapped (A in ethanol and B in THF) and separated (C in acetone). [CBr_4] in A to C: $1/2^n$ M from right to left (dilution times n = 0, 1, 2, 3...). Spectra (A-sub to C-sub) of specific solvent effect corresponding to halogen bonding are obtained by the spectral digital subtractions of the critical concentration absorption of CBr_4 from the experimental absorption curves over the critical concentration except for acetone. Alphabet presents concentration of CBr_4, for acetone, a, 0.0625 M; b, 0.125 M; c, 0.25 M; d, 0.50 M; e, 1.0 M. All other solvents, a, 1.2×10^{-5} M (general solvent effect); b, 0.03125 M; c, 0.0625 M; d, 0.125 M; e, 0.25 M. Insets: the lines are obtained by fitting the spot of A_{XBC} vs [CBr_4] at two different wavelengths.

TABLE 1: Absorptivity of the Complexes of CBr_4 and Solvents

complexes	methanol	ethanol	diethyl ether	THF	dioxane	acetone
wavelength/nm	285	290	293	299	302	326
absorptivity/$M^{-1}cm^{-1}$	1.2×10^2	1.2×10^2	1.1×10^2	0.90×10^2	1.0×10^2	0.074×10^2

Substituting mass balance expression for D, A, then obtains

$$K = \frac{\frac{A_{XBC}(t)}{\varepsilon b}}{\left(C_D - \frac{A_{XBC}(t)}{\varepsilon b}\right)\left(C_A - \frac{A_{XBC}(t)}{\varepsilon b}\right)} \quad (4)$$

given

$$\left(C_D - \frac{A_{XBC}(t)}{\varepsilon b}\right) = [D] \approx C_D$$

$$\frac{C_A}{A_{XBC}(t)} = \frac{1}{\varepsilon b} + \frac{1}{\varepsilon b K C_D} \quad (5)$$

where C_D and C_A are the primitive concentration of donor and acceptor; [D] and [A] are the equilibrium concentration of donor and acceptor, respectively; $A_{XBC}(t)$ is the instantaneous absorbance of XB complex [D•A]. The plots of the $A_{XBC}(t)$ versus C_A are linear, and the correlation coefficients of the resulting line are greater than 0.99; so, the 1:1 complex formed between donor and acceptor can be confirmed.[52]

As for each solvent, the plots of $A_{XBC}(t)$ versus corresponding concentration are drawn at two different wavelengths over 255 nm, as shown as inset in Figure 1A-sub−C-sub, respectively. All of the correlation coefficients are more than 0.99. These testify that CBr_4 formed 1:1 complexes with different solvents in certain concentration ranges, and the 1:1 complexes can be expressed as follows:

$$O + CBr_4 \rightleftharpoons [Br_3CBr\cdots O] \quad (6)$$

where O represents the oxygen-containing solvents. Generally, the CT complex can be formed between donor and acceptor dissolved in an inert solvent. Here, the oxygen-containing solvent acts as both medium and donor taking part in the formation of complex. So K and ϵ of a specific XB complex can not be separated from the Benesi−Hildebrand formulation. That is, it is difficult to obtain the values of K and ϵ by the intercept and slope of a routine fitted straight line from eq 5. Some attempts are made to get absorption spectra of the halogen bonding between carbon tetrabromide and oxygen atom in $CHCl_3$ inert solvent and produce the K and ϵ. No matter what the concentrations of CBr_4 or solvent are, when another component is titrated into solution gradually, the attempts are not successful. However, if we assume carbon tetrabromide interacts completely with solvent in 1:1 stoichiometry over the critical concentration, the absorptivity of the complexes can be estimated, as shown in Table 1.[53]

4.3. Mulliken Correlations of Charge-Transfer Energy. At present, σ_h really explain well the origination of halogen as charge or electron acceptor to participate in noncovalent interaction. However, the halogen bonding should involve the CT from an electron donor to σ^* of Br in C−Br bond rather than a simple electrostatic attraction between σ_h and electron donor under light radiation. In view of this point, the halogen bonding should obey the Mulliken correlations of charge-transfer energy to a certain extent.[54] The energy of the photoelectrical transition of donor−acceptor complexes is determined primarily by their HOMO/LUMO separations that are evaluated via redox potential in solution or ionization potential/electron affinity in the gas phase. As such, the energies ($h\nu_{CT}$) of absorption bands of a related series of molecular complexes sharing a common acceptor must be linearly dependent on the oxidation potential of the donor and vice versa.[55] Accordingly, the electrical properties of complexes of carbon tetrabromide with six organic solvents are considered. The oxidation potentials (average value) are quantitatively extracted as the cyclic voltammetric peak potentials (E^o_{pa}, V vs SCE) except for dioxane and diethyl ether because the supporting electrolyte ($NBu_4^+PF_6^-$) is not soluble in both solvents. CV oxidation waves (average value) of solvents are measured at 0.929 V for methanol, 0.886 V for ethanol, 0.823 V for THF, and 0.732 V for acetone, respectively.

Figure 2 demonstrates the linear dependence of the oxidation potentials with the absorption energy for a series of carbon tetrabromide complexes. The linear correlations of these anodic potentials with the spectral energies of the four organic solvent complexes establish the high concentration-dependent charge-transfer character of the CBr_4−solvent associations.

It can be concluded that the Mulliken relationship implies that the stronger the nucleophile, the higher the interaction energy can be expected for σ_h bonded complex. The higher the electronegativity, the greater is the attraction of lone pair.[56] Also, CT interaction may be an un-negligible even dominant factor sometimes. For example, an early viewpoint supported that the iodine−halogen interaction is described to transfer of lone pair of donor to σ^*-orbital of X-I bond.[57]

4.4. Theoretical Calculation Results. The structures of all complexes and monomers are fully optimized at the B3PW91/6-311+G(3df,2p) level. The MP2/6-311+G(3df,2p) calculations are performed on the formation of complexes between carbon tetrabromide and oxygen-containing organic solvents.

4.4.1. Stationary Geometry of C−Br···O Complexes. Some structural and energetic properties of similar complexes have

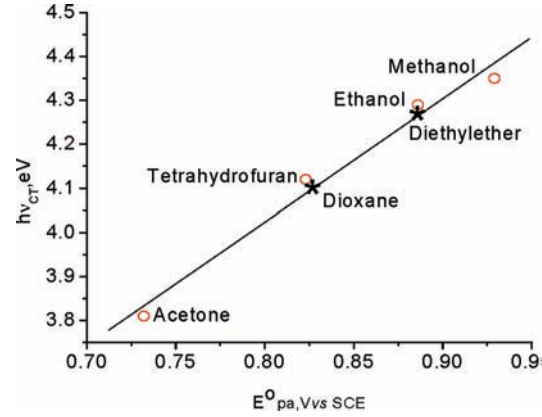

Figure 2. Mulliken correlations between the energies of CT bands and the oxidation potentials of the donors in the complexes of CBr_4 acceptor. For dioxane and diethyl ether, the plots could be theoretically speculated to locate the positions indicated by symbol star in this figure.

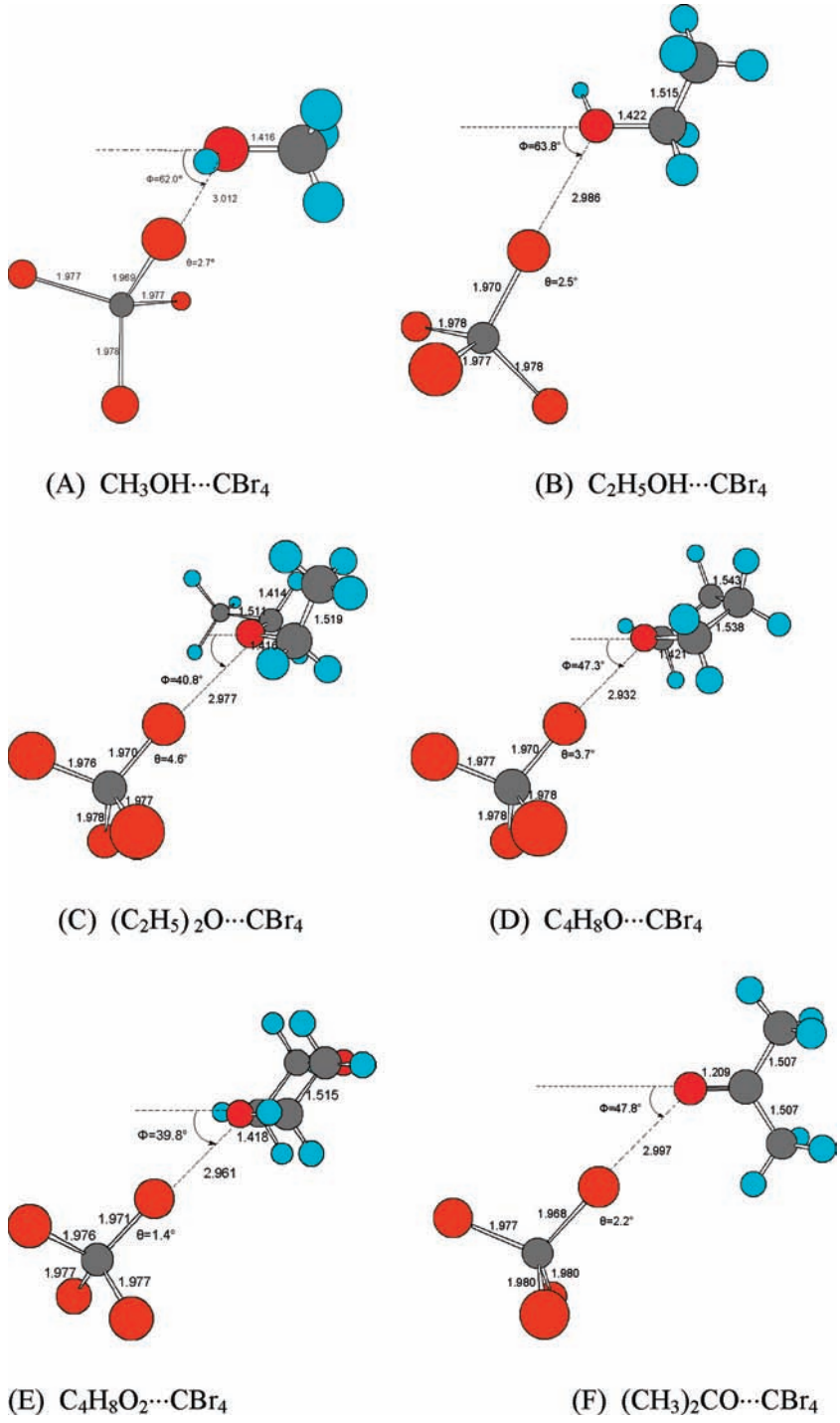

Figure 3. B3PW91/6-311+(3df,2p) optimized main geometrical parameters (in Å and degree) of the complexes: (A) $CH_3OH\cdots CBr_4$, (B) $C_2H_5OH\cdots CBr_4$, (C) $(C_2H_5)O\cdots CBr_4$, (D) $C_4H_8O\cdots CBr_4$, (E) $C_4H_8O_2\cdots CBr_4$ and (F) $(CH_3)CO\cdots CBr_4$.

been calculated by Ananthavel et al.[56] and Riley et al.[58] In this work, the complexes have been confirmed first by experiments aforementioned, and it is found by calculation that the optimum halogen bond angle is generally within the range from 175.4° to 178.6°, corresponding to an interaction between the halogen σ_h and the lone pair of electrons on oxygen. Figure 3 shows the optimized structure of the carbon tetrabromide and solvent molecule complex. In Figure 4, the Br atom is positioned in such a way that its σ_h can interact with the lone pair electrons on the oxygen atom of solvent molecules. Table 2 gives the important geometric parameters for the halogen bonding complexes. The optimized angle of C−Br···O is consistent with typical "head-on" halogen bonding interaction model,[4,59,60] and agrees with the crystal structures.[55]

All optimized C−Br···O distances are within sum of van der Waals radii, 3.35 Å, which reveals the existence of the weak halogen-bonding interaction between bromine and oxygen atoms. The C−Br···O distances in crystal structure between CBr_4 and oxygen-containing solvents could not be found up to date. While the Br−Br···O distances can be found in references, for example, 2.71 Å in 1,4-dioxane-Br_2 crystal, 2.82 Å in acetone-Br_2 crystal, 2.78 Å (2.71 Å) in methanol-Br_2 (bis-(methanol)-Br_2) crystal, 3.21 Å in dioxane-oxalyl bromide crystal, 3.2 Å calculated in formaldehyde-halobenzene com-

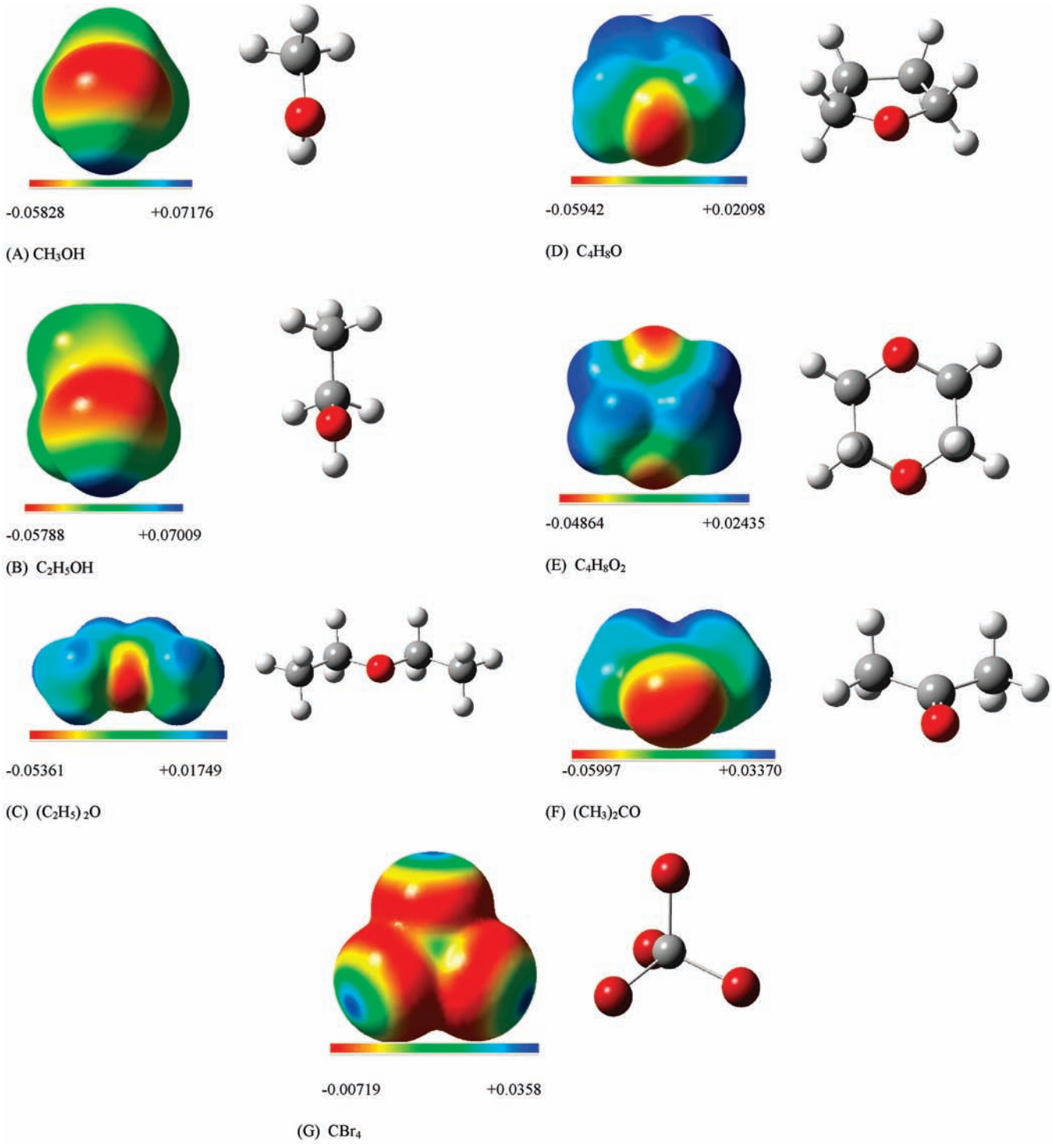

Figure 4. Electrostatic potential mapped on the surface of molecular electron density at the 0.001 electrons Bohr^{-3}. The maximum electrostatic potentials of oxygen atom and Br are listed in Table 3. The color ranges (in a.u.) from red to blue are shown in color scale bar.

TABLE 2: Geometric Parameters of Halogen Bonding Complexes Computed at B3PW91/6-311+G(3df,2p) Level

complexes	$d_{Br\cdots O}$ (Å)	C−Br···O angle (°)
CBr_4 + methanol	3.012	177.3
CBr_4 + ethanol	2.986	177.5
CBr_4 + diethyl ether	2.977	175.4
CBr_4 + THF	2.932	176.3
CBr_4 + dioxane	2.961	178.6
CBr_4 + acetone	2.997	177.8

plex,[34,35,55,58,61] respectively. In Table 2, the Br···O distances obtained by the present theoretical calculation in gas phase are apparently larger than the above values in different crystals, but less than 3.2 Å. Both calculated distance and bonding angles seem to be acceptable.

4.4.2. Interaction Energies Calculated Based on Surface Electrostatic Potentials of C−Br···O Complexes. The surfaces electrostatic potentials of targeted molecules are shown in Figure 4. Table 3 lists the most positive surface electrostatic potentials $V_{S,max}$ of Br atom in carbon tetrabromide and the most negative surface electrostatic potentials $V_{S,min}$ of oxygen atom in oxygen-containing organic solvents. It can be seen that there is a positive σ_h along the extension of C−Br bond. The positive region can

TABLE 3: Halogen Bond Interaction Energies ΔE and Changes in Vibration Frequency $\Delta\omega$ Computed by the B3PW91/6-311+G(3df,2p) Where the Bond Length Changes ΔR Are Based on the Surface Electrostatic Potentials Calculated by B3PW91/6-31+G(d)

	V*s* of oxygen [a]	ΔE (kcal/mol)		changes in bond properties		
complexes	kcal/mol	B3PW91	MP2[b]	bond	$\Delta\omega$,cm^{-1}	ΔR, Å
CBr_4 + methanol	−36.6	−1.6	−2.27	C−Br	11	−0.0028
CBr_4 + ethanol	−36.3	−1.76	−2.13	C−Br	11	−0.0024
CBr_4 + aether	−33.6	−0.26	−0.46	C−Br	9	−0.0028
CBr_4 + THF	−37.3	−5.13	−5.6	C−Br	10	−0.0025
CBr_4 + dioxane	−30.5	−1.86	−2.61	C−Br	9	−0.0023
CBr_4 + acetone	−37.7	−1.88	−2.64	C−Br	12	−0.0062

[a] To CBr_4, the maximum SEP was denoted as *Vs*, max, 22.5 kcal/mol, to other reactants the minimum SEP was denoted as *Vs*, min, and all the *Vs*, max/min are on the 0.001 electrons/Bohr^3 surface of halogens Br in complex. [b] The MP2 energies were calculated at the B3PW91 optimized geometries.

TABLE 4: Experimental Excitation Energies and Theoretical Computed CT Vertical Excitation Energies (in eV)

	experimental		TD-B3PW91/6-31+G(d)	
complexes	E_{ABS} (nm/eV) [a]	oxidation potentials (V)	excited state	T_v (*f*) (eV)
CBr_4 + methanol	285/4.35 $\underline{305}$[b]/4.06	0.929	S_4	4.413 (0.0686)
CBr_4 + ethanol	290/4.29 $\underline{310}$[b]/4.00	0.886	S_4	4.367 (0.0775)
CBr_4 + diethyl ether	293/4.26 $\underline{304}$[b]/4.08		S_5	4.656 (0.0219)
CBr_4 + THF	299/4.15 $\underline{306}$[b]/4.05	0.823	S_4	3.908 (0.0388)
CBr_4 + dioxane	302/4.12 $\underline{310}$[b]/4.00		S_5	4.572 (0.0257)
CBr_4 + acetone	326/3.81 327[b]/3.79	0.732	S_4	3.892 (0.0477)

[a] λ_{ABS}, absorption wavelengths corresponding to 0.0625 M CBr_4; [b] $\underline{\lambda}$: estimated wavelengths according to extreme concentration of CBr_4.

TABLE 5: Electronic Coupling Element of Halogen-Bonding Complexes[a]

complexes	methanol	ethanol	diethyl ether	THF	dioxane	acetone
υ_{CT} /nm/cm^{-1}	285/35088	290/34483	293/34130	299/33445	302/33113	326/30675
υ_{fwhm}/cm^{-1}	4471	4985	4507	2568	2671	2261
H_{DA}/cm^{-1}	968	991	894	618	654	156

[a] The υ_{CT} and $\upsilon_{1/2}$ corresponding to 0.0625 M carbon tetrabromide; H_{DA}= $0.0206(\upsilon_{CT}\Delta\upsilon_{1/2}\epsilon_{CT})^{1/2}/R_{DA}$[42,61] ϵ_{CT} and R_{DA}(Å) taken from Tables 1 and 2. υ_{FWHM} = full width at half-max.

interact electrostatically with negative regions on oxygen-containing organic molecules, forming σ_h-bond. For example, the Br in CBr_4 has $V_{S,max}$ of 22.5 kcal/mol, and $V_{S,min}$ of O in methanol is −36.6 kcal/mol, so they can interact attractively. As shown in Table 3, the interaction energies are all negative, which indicates thermodynamic stability of the complexes is achievable.

4.4.3. CT Characteristics, Vertical Excitation Energies (T_v) and Electronic Coupling Elements (H_{DA}). The absorption spectra and Mulliken relationship mentioned above have confirmed the CT characteristics of the complexes. Table 4 lists the T_v values of complexes and the corresponding oscillator strengths, *f*. TD-DFT calculated T_v values are consistent with the corresponding UV−Vis spectra of these complexes measured in this work. For example, the UV−Vis absorption peak of $(CH_3)_2CO\cdots BrCBr_3$ at 326 nm (3.81 eV) corresponds well to the result of vertical excitation wavelength 319 nm (3.89 eV). Although the T_v values of $(C_2H_5)_2O\cdots BrCBr_3$ and $C_4H_8O_2\cdots CBr_4$ do not meet the peak values of UV−Vis absorption spectra, they are also within the UV−Vis absorption bands. The difference can be a result of the fact that the experiments were performed in solution, but theoretical calculation in gas phase.

Based on the experimental data and calculated Br···O distances, the electronic coupling elements (H_{DA}) are calculated and listed in Table 5. According to Kochi,[62] the H_{DA} values show that the halogen-bonding complexes between CBr_4 and solvents should be localized or partially delocalized in the cases of all others. It can be confirmed that the CT really occurred, but it should be weak in accordance with the criterions proposed by Kochi.[62] The conclusion in interaction strength is coordinated between the H_{DA} values and the interaction energies based on surface electrostatic potentials.

4.4.4. Blue-Shifted Br···O Bonding. Table 3 and Figure 4 show that the C−Br bond length decreases and the vibration frequency increases. Usually, halogen bonding is the red-shift type,[56] as the blue-shift type is rare.[10] However, here the calculation shows that Br···O is a blue-shift type. The distance of C−Br is shortened by −0.0062 to −0.0023 Å and vibration frequency is increased by 9 to 12 cm^{-1}, similar to that reported by Murray.[10] From H_{DA}, CT is really weak. So, the σ_h-bonding, that is, electrostatic attraction, may be a dominant factor among other possible factors including the charge-transfer, dispersion force, and electrostatic attraction. Further insight into the contribution of each force to halogen bonding is currently being explored in our group.

5. Conclusions

The experimental and computational methods are all performed to investigate the characters of 1:1 complexes between CBr_4 with methanol, ethanol, diethyl ether, tetrahydrofuran, dioxane, and acetone. Experimental results indicate that high concentration-dependent halogen bonding, specific solvent effect, exists when the concentration of CBr_4 is over the critical concentration range and the XB complex has CT characteristic. The calculation of surface electrostatic potential shows that Br has a positive σ_h; thus, the electrostatic abstraction between the σ_h and the oxygen may be a more important factor to form a halogen-bonding complex. Also, the Br···O halogen bonding

are of the blue-shift type. The contribution of each force to halogen bonding is being investigated in our group.

Acknowledgment. This work is financially supported by the National Natural Science Foundation of China (No. 20675009) and the Natural Science Foundation of Beijing (No. 2093037). Authors thank Mr. Wei Cao and Dr. Chang Zheng Wang for their help in CV measurement. Authors also appreciate very much the valuable suggestions and sincere help in theoretical calculation from Dr. and associate professor Ya Jun Liu.

References and Notes

(1) Metrangolo, P.; Neukirch, H.; Pilati, T.; Resnati, G. *Acc. Chem. Res.* **2005**, *38*, 386–395, and refs therein.

(2) Politzer, P.; Lane, P.; Concha, M. C.; Ma, Y. G.; Murray, J. S. *J. Mol. Model.* **2007**, *13*, 305–311, and refs therein.

(3) Legon, A. C. *Chem.—Eur. J.* **1998**, *4*, 1890–1897.

(4) Legon, A. C. *Angew. Chem., Int. Ed.* **1999**, *38*, 2686–2714.

(5) Politzer, P.; Murray, J. S.; Lane, P. *Int. J. Quantum Chem.* **2007**, *107*, 3046–3052.

(6) Murray, J. S.; Lane, P.; Politzer, P. *Int. J. Quantum Chem.* **2007**, *107*, 2286–2292.

(7) Clark, T.; Hennemann, M.; Murray, J, S.; Politzer, P. *J. Mol. Model.* **2007**, *13*, 291–296.

(8) Murray, J. S.; Lane, P.; Clark, T.; Politzer, P. *J. Mol. Model.* **2007**, *13*, 1033–1038.

(9) Politzer, P.; Murray, J. S.; Concha, M. C. *J. Mol. Model.* **2008**, *14*, 659–665.

(10) Murray, J. S.; Concha, M. C.; Lane, P.; Hobza, P.; Politzer, P. *J. Mol. Model.* **2008**, *14*, 699–704.

(11) Riley, K. E.; Hobza, P. *J. Chem. Theory Comput.* **2008**, *4*, 232–242.

(12) Lucassen, A. C. B.; Vartanian, M.; Leitus, G.; van der Boom, M. E. *Cryst. Growth Des.* **2005**, *5*, 1671–1673.

(13) Metrangolo, P.; Meyer, F.; Pilati, T.; Proserpio, D. M.; Resnati, G. *Chem.—Eur. J.* **2007**, *13*, 5765–5772.

(14) Walsikwska, A.; Gdaniec, M.; Połoñski, T. *Cry. Eng. Commun.* **2007**, *9*, 203–206.

(15) Chowdhury, M.; Kariuki, B. M. *Cryst. Growth Des.* **2006**, *6*, 774–780.

(16) Chu, Q. L.; Wang, Z. M.; Huang, Q. C.; Yan, C. H.; Zhu, S. Z. *J. Am. Chem. Soc.* **2001**, *123*, 11069–11070.

(17) Fourmigué, M.; Batail, P. *Chem. Rev.* **2004**, *104*, 5379–5418.

(18) Zhu, S. Z.; Xing, C. H.; Xu, W.; Jin, G. F.; Li, Z. T. *Cryst. Growth Des.* **2004**, *4*, 53–56.

(19) Metrangolo, P.; Meyer, F.; Pilati, T.; Proserpio, D. M.; Resnati, G. *Cryst. Growth Des.* **2008**, *8*, 654–659.

(20) Bruce, D. W.; Metrangolo, P.; Meyer, F.; Präsang, C.; Resnati, G.; Terraneo, G.; Whitwood, A. C. *New J. Chem.* **2008**, *32*, 477–482.

(21) Nguyen, H. L.; Horton, P. N.; Hursthouse, M. B.; Legon, A. C.; Bruce, D. W. Halogen Bonding: A New Interaction for Liquid Crystal Formation. *J. Am. Chem. Soc.* **2004**, *126*, 16–17.

(22) Xu, J. W.; Liu, X. M.; Lin, T. T.; Huang, J. H.; He, C. B. *Macromolecules* **2005**, *38*, 3554–3557.

(23) Auffinger, P.; Hays, F. A.; Westhof, E.; Ho, P. S. *Proc. Natl. Acad. Sci. U.S.A.* **2004**, *101*, 16789–16794.

(24) Voth, A. R.; Hays, F. A.; Ho, P. S. *Proc. Natl. Acad. Sci. U.S.A.* **2007**, *104*, 6188–6193.

(25) Metrangolo, P.; Resnati, G. *Science* **2008**, *321*, 918–919.

(26) Price, S. L.; Stone, A. J.; Lucas, J.; Rowland, R. S.; Thornley, A. E. *J. Am. Chem. Soc.* **1994**, *116*, 4910–4918.

(27) Mitchell, J. B. O.; Price, S. L.; Leslie, M.; Buttar, D.; Roberts, R. J. *J. Phys. Chem. A* **2001**, *105*, 9961–9971.

(28) Zordan, F.; Brammer, L.; Sherwood, P. *J. Am. Chem. Soc.* **2005**, *127*, 5979–5989.

(29) Awwadi, F. F.; Willett, R. D.; Peterson, K. A.; Twamley, B. *Chem.—Eur. J.* **2006**, *12*, 8952–8960.

(30) Day, G. M.; Price, S. L. *J. Am. Chem. Soc.* **2003**, *125*, 16434–6443.

(31) Rosokha, S. V.; Neretin, I. S.; Rosokha, T. Y.; Hecht, J.; Kochi, J. K. *Heteroatom Chem.* **2006**, *17*, 449–459.

(32) Bosch, E.; Barnes, C. L. *Cryst. Growth Des.* **2002**, *2*, 299–302.

(33) Reddy, C. M.; Kirchner, M. T.; Gundakaram, R. C.; Padmanabhan, K. A.; Desiraju, G. R. *Chem.—Eur. J.* **2006**, *12*, 2222–2234.

(34) Bent, H. A. *Chem. Rev.* **1968**, *68*, 587–648.

(35) Hassel, O.; RØmming, C. *Quart Rev.(London)* **1962**, *16*, 1–18.

(36) Truong, T. B. *J. Phys. Chem.* **1980**, *84*, 964–970.

(37) Pal, S. K.; Zhao, L.; Zewail, A. H. *Proc. Natl. Acad. Sci. U.S.A.* **2003**, *100*, 8113–8118.

(38) Derossi, S.; Brammer, L.; Hunter, C. A.; Ward, M. D. *Inorg. Chem.* **2009**, *48*, 1666–1677.

(39) Wash, P. L.; Ma, S. H.; Obst, U.; Rebek, J. *J. Am. Chem. Soc.* **1999**, *121*, 7973–7974.

(40) Rosokha, S. V.; Kochi, J. K. *Struct. Bonding (Berlin)* 2008, *126*, 137−160.

(41) Carbon tetrabromide is easy to dissociate to produce bromine in investigated solvents except for dioxane and tetrahydrofuran, making the solution yellow in ambient light, which is testified by KI−starch experiment. Among four solvents in which bromine is dissociated more easily, the color of ethanol solution changes immediately as soon as the carbon tetrabromide dissolved totally and deepens with standing time. Fortunately, the spectral tail at 350−450 nm caused by bromine vanishes quickly with the solution being diluted. The other three solvents stay colorless for about 30 min in experimental conditions and remain colorless for a much longer time. All experiments can be completed successfully in dark. Possible mechanism should be that CBr_4 produce Br_2C:carbene and Br_2 in ethanol under ambient light, then Br_2C reacts with ethanol to produce $CH_3CH_2OCHBr_2$. The addition of excessive KI and soluble starch into solution make the system blue because of oxidation of Br_2.

(42) Lindeman, S. V.; Hecht, J.; Kochi, J. K. *J. Am. Chem. Soc.* **2003**, *125*, 11597–11606.

(43) Parr, R. G.; Yang, W. *Density-functional theory of atoms and molecules*; Oxford University Press: Oxford, 1989.

(44) Becke, A. D. *J. Chem. Phys.* **1993**, *98*, 5648–5652.

(45) Perdew J. P. *In Electronic Structure of Solids '91*; Ziesche, P., Eschrig, H., Eds.; AkademieVerlag: Berlin, 1991; p11.

(46) Wadt, W. R.; Hay, P. J. *J. Chem. Phys.* **1985**, *82*, 270–283.

(47) Clark, T.; Chandrasekhar, J.; Schleyer, P. V. R. *J. Comput. Chem.* **1983**, *4*, 294–301.

(48) Sæbo, S.; Almlöf, J. *Chem. Phys. Lett.* **1989**, *154*, 83–89.

(49) Bauernschmitt, R.; Ahlrichs, R. *Chem. Phys. Lett.* **1996**, *256*, 454–464.

(50) Frisch, M. J.; Trucks, G. W.; Schlegel, H. B.; Scuseria, G. E.; Robb, M. A.; Cheeseman, J. R.; Montgomery, J. A.; Vreve, N. T.; Kudin, K. N.; Burant, J. C.; Millam, J. M.; Iyengar, S. S.; Tomasi, J.; Barone, V.; Mennucci, B.; Cossi, M.; Scalmani, G.; Rega, N.; Petersson, G. A.; Nakatsuji, H.; Hada, M.; Ehara, M.; Toyota, K.; Fukuda, R.; Hasegawa, J.; Ishida, M.; Nakajima, T.; Honda, Y.; Kitao, O.; Nakai, H.; Klene, M.; Li, X.; Knox, J. E.; Hratchian, H. P.; Cross, J. B.; Adamo, C.; Jaramillo, J.; Gomperts, R.; Stratmann, R. E.; Yazyev, O.; Austin, A. J.; Cammi, R.; Pomelli, C.; Ochterski, J. W.; Ayala, P. Y.; Morokuma, K.; Voth, G. A.; Salvador, P.; Dannenberg, J. J.; Zakrzewski, V. G.; Dapprich, S.; Daniels, A. D.; Strain, M. C.; Farkas, O.; Malick, D. K.; Rabuck, A. D.; Raghavachari, K.; Foresman, J. B.; Ortiz, J. V.; Cui, Q.; Baboul, A. G.; Clifford, S.; Cioslowski J.; Stefanov, B. B.; Liu, G.; Liashenko, A.; Piskorz, P.; Komaromi, I.; Martin, R. L.; Fox, D. J.; Keith, T.; Al-Laham, M. A.; Peng, C. Y.; Nanayakkara, A.; Challacombe, M.,; Gill, P. M. W.; Johnson, B.; Chen, W.; Wong, M. W.; Gonzalez, C.; Pople, J. A.; Gaussian, Inc.: Pittsburgh, PA, 2003.

(51) Benesi, H. A.; Hildebrand, J. H. *J. Am. Chem. Soc.* **1949**, *71*, 2703–2707.

(52) Blackstock, S. C.; Lorand, J. P.; Kochi, J. K. *J. Org. Chem.* **1987**, *52*, 1451–1460.

(53) Stevenson, D. P.; Coppinger, G. M. *J. Am. Chem. Soc.* **1962**, *84*, 149–152.

(54) Mulliken, R. S. *J. Am. Chem. Soc.* **1952**, *74*, 811–824.

(55) Pennington, W. T.; Hanks, T. W.; Arman, H. D. "Halogen Bonding with Dihalogens and Interhalogens" (p 73) andMetrangolo P. Resnati G. Pilati T., Biella S. "Halogen Bonding in Crystal Engineering" (p 144) in "Halogen Bonding Fundamentals and Applications"; Metrangolo, P., Resnati, G., Eds.; *Struct. Bonding (Berlin)* 2008, *126*, 65, Springer.

(56) Mohajeri, A.; Pakiari, A. H.; Bagheri, N. *Chem. Phys. Lett.* **2009**, *467*, 393–397.

(57) Ananthavel, S. P.; Manoharan, M. *Chem. Phys.* **2001**, *269*, 49–57.

(58) Riley, K. E.; Murray, J. S.; Politzer, P.; Concha, M. C.; Hobza, P. *J. Chem. Theory Comput.* **2009**, *5*, 155–163.

(59) Lommerse, J. P. M.; Stone, A. J.; Taylor, R.; Allen, F. H. *J. Am. Chem. Soc.* **1996**, *118*, 3108–3116.

(60) Ramasubbu, N.; Parthasarathy, R.; Murray-Rust, P. *J. Am. Chem. Soc.* **1986**, *108*, 4308–4314.

(61) Riley, K. E.; Merz, K. M., Jr. *J. Phys. Chem. A* **2007**, *111*, 1688–1694.

(62) Rosokha, S. V.; Kochi, J. K. *Acc. Chem. Res.* **2008**, *41*, 641–653.

JP905914Q